Computational and experimental analysis of highly isolated double side triple band notched UWB MIMO antenna

Prabhu Palanisamy* **and Malarvizhi Subramani†**

Department of ECE, SRM Institute of Science and Technology, Katankulatur, Chennai, 603203, Tamilnadu, India

Abstract

In this article, we present a double side highly isolated triple band notched UWB MIMO antenna for short-range wireless communication applications. The proposed MIMO antenna design provides a UWB band with the notched band at the IEEE INSAT C band satellite communication and WLAN band (4.6–5.9 GHz), the X band up link and down link satellite communication (7.70–8.43) and (10.3-10.98 GHz). It has double side placement of polygon-shaped radiating elements, and an inverted L-shaped stub to obtain high isolation between radiating elements. The proposed antenna has a size of 18 $\times$ 28 mm2, which operates from 3 to 12 GHz. The antenna characteristics such as isolation between radiating elements, S11/S22, gain, and radiation characteristics are studied. The proposed MIMO antenna has isolation of >19 dB, 0-7.5 dBi peak gain and almost radiation pattern over the entire operating frequency band with pattern diversity. Furthermore, MIMO diversity performance was investigated using an ECC, diversity gain, multiplexing efficiency, TARC, and CCL. The proposed UWB MIMO antenna has very low ECC of 0.0025, and DG of >9.9, over the entire operating band (3-12 GHz). Also, the real-time indoor short range communication capability of the proposed MIMO antenna demonstrated by using the NI 802.1 framework.

Key words: Double side antenna, MIMO antenna, Compact MIMO antenna, Notched band, Triple notched band, NI802.11 Framework

1 Introduction

Due to the tremendous development of wireless communication systems, there is a need for high data rates, strong reliability, low power consumption, and robustness without multi-path fading and interference [1]. With FCC, the frequency range allocated to UWB

*E-mail: prabhusrm2015@gmail.com

†E-mail: malarvizhi.g@ktr.srmuniv.ac.in

applications is 3.1-10.6 GHz. UWB Systems has many advantages, but multi-path fading is a significant problem [2]. Thus, a UWB multiple-input-multiple-output system gives a solution to Multipath fading and interference. In addition, importantly, MIMO systems increase channel capacity and data rate without using additional bandwidth and power. [1]. However, MIMO antenna design has some challenges such as size and mutual coupling between radiating elements, as modern portable devices are compact and packed tightly [3]. Therefore, it is still required to reduce mutual coupling while achieving miniaturization in MIMO antenna systems. Recently, considerable effort has been addressed to reduce the mutual coupling in UWB MIMO antennas [1–30]. Another critical problem in the UWB antenna is narrowband interference. The band notch characteristics provide a solution to the narrowband interference [16–23]. Two circular shaped monopole antennas isolated using unipolar EBG structure and it resonated from 3-18 GHz [3]. Mushrooms and Uniplanar plus shaped EBG structures are used to obtain band notch for WiMAX, WLAN, and X-band frequencies. The mutual coupling among the monopole antennas is achieved by employing the slotted ground in [4]. The triangular slots were removed from the top and bottom of the patch to obtain wide band matching in [5]. In [6], to obtain UWB MIMO characteristics, the two triangular radiating elements are fed by a tapered microstrip. The two-notch frequencies obtained by removing, two L-shaped(inverted) slots on the radiator which operate on the 2.93-20 GHz band. The antenna consists of two P-shaped radiators which are 180$\circ$ laterally and spatially opposite each other with a spacing of 0.075 λo. The two crescent-like slots and the rectangular strips are roughened on both sides of the grooved P-shaped radiators to obtain bandwidth of 2.5 to 12 GHz. Isolation was achieved in [7] by introducing a mesh-like metal strip and a triangular slot. The MIMO antenna is composed using two same square patches at 2.4 GHz. An H-shaped defective ground geometry is used for isolation and cross polarization in [8]. An identical planar UWB radiator and non-identical feeding scheme used for size and mutual coupling reduction in [11]. In [12], a two-element MIMO antenna implemented with two λ/4 wavelength microstrip slot antenna elements for WLAN applications and high isolation obtained through the defective ground(DG). A MIMO antenna consisting of two eye-shaped radiating elements and an extruded T-stub partial ground is used to improve isolation [13]. In [14], double side MIMO antenna proposed with four polygon-shaped monopole radiators with dimensions of 30 x 30 mm^2. The use of a double-sided EBG structure improves isolation and has bandwidth of 3-11 GHz. A 40$\times$40 mm^2 four-circle monopole element array is placed on bottom and top sides of the substrate, and the working frequency is 3.1-11.0 GHz, and the isolation >15 dB in [15]. In, [16] The dual notch band (WLAN and X band) is realized with a Vivaldi antenna using SRR, and inter-port isolation is achieved by removing the T-shaped groove in the ground plane. The triple-notch feature was achieved using the multi-slot and slit method in [17]. The isolation between the ports enhanced by the two-sided identical layout and a defective ground. Two U shaped slots and SRR slot used to reject the WLAN, WiMAX and X band in [19] The WLAN(5.5GHz) and WIMAX (3.5GHz) bands are notched in [20] by inserting SRR into the feed line of the UWB antenna. The inverted U-shaped half-wavelength resonator inserted at the CPW feed to reject WLAN(5.5 GHz), band in [22]

[Table 1 about here.]

Although many MIMO antennas and isolation methods with different geometries are implemented with notch characteristics for UWB antenna applications. Future portable devices still require MIMO antenna designs with further miniaturization and high isolation. In this article, the two-port double side placement of the radiator and inverted L-shaped decoupling structure are introduced. It comprehends two polygon radiators on both sides of the substrate. A simple inverted L-shaped stub structure extruded both sides on a partial ground plane to achieve high isolation between the ports.
Furthermore, triple band notch characteristics achieved by removing Inverted L-shaped slot on radiators and split ring resonator (SRR). The proposed antenna design provides UWB band with notched band at IEEE INSAT C band satellite communication and WLAN band (4.6–5.9 GHz), and the X band uplink and downlink satellite communication (7.70–8.43 GHz and 10.3-10.98 GHz). With the miniaturization of 18 x 28 mm^2, the double side decoupling structure provides high isolation, >19 dB(S21 / S12) between the ports. It has excellent impedance matching, high isolation, and MIMO performance compare to the existing MIMO antennas.

[Figure 1 about here.]

The structure of this paper is as follows: UWB antenna design and three-band notch characteristics discussed in Section 2. Section 3 provides the equivalent circuit for the notch resonators. Section 4 describes the design process of UWB MIMO. Simulation and measurement results are discussed in Section 5. Radiation characteristics are discussed in Section 6. Similarly, Section 7 explains the MIMO performance. Section 8 gives a comparison of the proposed MIMO antenna with recently published MIMO antennas. Real time validation addressed in section 9. Section 10 summarizes the proposed MIMO antenna performance.

2 Antenna configuration

2.1 Single polygon-shaped monopole antenna

In this article, we have proposed a double side placement of monopole radiators with triple-band notch characteristics and improved isolation for two-port MIMO antenna. Compared with the existing dual-port MIMO antennas, the proposed method has following novelty and advancement, double placement methodology with the triple-band notch characteristics, a compact size, and high isolation as shown in table 1. The fundamental structure of single element polygon-shaped antenna is designed with a 12 x 8 mm^2 size as presented in Figure 1. The proposed polygon-shaped radiator created by removing the triangular slot on the two bottom edges of the polygon-shaped radiators, which results in impedance matching and bandwidth enhancement. The miniaturized design of the UWB antenna can be achieved using a monopole structure, and the following Equation (1) can

approximate the resonant frequency of the proposed polygon-shaped monopole antenna.

$$f_r = \frac{14.4}{l_1 + l_2 + g + \frac{B_1}{2\pi\sqrt{\epsilon_r + 1}} + \frac{B_2}{2\pi\sqrt{\epsilon_r + 1}}} \tag{1}$$

The area of the ground plane is B_1, and the radiating patch is B_2. The lengths of the partial ground and the polygon-shaped radiators are l_1 and l_2, respectively. The distance from radiator bottom and the top of the partial ground is 'g.' The polygon-shaped monopole antenna is chosen because of the advantages of polygon-shaped monopole antennas such as the broad operating band and excellent radiation characteristics [5]. The proposed arrangement provides impedance matching via a 1.85 mm wide microstrip line. Also, For the bandwidth improvement, the inverted L-shaped partial ground plane is utilized. The antenna substrate width and dielectric constant were 1.6 mm and 4.4, respectively. This can be confirmed from the S11 diagram shown in Figure 1(b). Resonance has occurred in the 3 to 12 GHz range with S11/S22 of < -10 dB.

2.2 Design theory of triple notch band

The triple-band rejection characteristics achieved in the proposed antenna by using the following steps

Step 1: The fundamental structure of the monopole radiator (Radiator 1) comprises polygon-shaped radiator and an inverted L-shaped ground to achieve ultra-wideband characteristics of 3 to 12 GHz, S11 <-10 dB, as shown Figure 4.

Step 2: In order to avoid the narrow band interference, IEEE INSAT C band satellite communication (4.6-4.9 GHz) and WLAN band (5–5.9 GHz) band frequencies are suppressed from UWB by removing the upper L-shaped slot on the Radiator 2 as shown Figure 2(b). Equation (2) illustrates that adjusting the value of an L-shaped slot parameter (L_{up}, W_{up}, g_{up}) provides the notch of IEEE INSAT C band satellite communication (4.6-4.9) and WLAN band (5–5.9 GHz) band. As shown in the Figure 4, when the L slot of the radiator is removed the impedance of the feed and the radiator do not match, so the band notch characteristic is realized.Figure 4. As can be seen from the figure, the reflection coefficients of the notch band (4.6-4.9 GHz) and WLAN (5-5.9 GHz) are very poor, that is, S11 > -3 dB. In order to effectively display the performance of the notch structure, the VSWR of the notch is shown in Figure 14.

$$F_{n1} = \frac{c}{2\sqrt{\varepsilon_{eff}}\,(2 * (L_{up} + W_{up}) - g_s)} \tag{2}$$

Step 3: In the subsequent method, two SRR are stacked on the left and right sides of the feed line to reject the X- band uplink and downlink satellite communication (10.3-10.98 GHz), frequency band, as shown in Figure 2(c) (Radiator 3). Furthermore, the insertion of SRR leads to an impedance mismatch at higher frequencies. In order to achieve impedance matching, a semicircle shaped slot is removed at the feed line as shown in Figure 2(c). The reflection coefficient of the radiator 3 is presented in Figure 4. It can be perceived from the Figure 4 at the notched band (10.5 GHz) the return loss is very poor, i.e., S11>-5 dB. This notch band is controlled by changing the values of the

geometric parameters(L_{Sr}, W_{Sr}, g_{Sr}, L_1 and L_2) as inEquation (3). Figure 14 shows the VSWR of the 10.5 GHz-band notch, which effectively shows the performance of the notch structure.

$$F_{n2} = \frac{c}{2\sqrt{\varepsilon_{eff}}\,(2 * (L_{sr} + W_{sr}) - g_{sr})} \tag{3}$$

Step 4: The X band up link and down link satellite communication (7.70–8.43 GHz) band-notch obtained by removing lower L-shaped slot on the lower side of the radiator 3 as shown in Figure 2 (Radiator 4). Equation (4) Illustrates that the band notch of X- band (7.70–8.43 GHz) frequency achieved by tuning the parameters of the lower L-shaped (L_{lw}, W_{lw}, and g_s). As shown in the figure, when the lower L slot of the radiator is removed the impedance of the feed and the radiator do not match, so the band notch characteristic is realized at (7.70–8.43) GHz, as presented in Figure 4. It is perceived that from the Figure 4, the reflection coefficient at X band (7.70–8.43 GHz) frequency is very poor, i.e., S11>-3dB. Figure 14 shows the VSWR for an X-band notch to demonstrate the performance of the notch structure effectively. Eventually, form the Figure 4 the proposed radiator(Radiator 4) has UWB impedance bandwidth from 3-12 GHz with <-10 dB reflection coefficients but S11 at notch frequencies (4.6-5.9 GHz, 7.70–8.43 GHz and 10.3-10.98 GHz) is >-5 dB.

$$F_{n3} = \frac{c}{2\sqrt{\varepsilon_{eff}}\,(2 * (L_{lw} + W_{lw}) - g_s)} \tag{4}$$

$$\varepsilon_{eff} = \frac{\varepsilon_{r+}1}{2} \tag{5}$$

Where 'c' is the velocity of light, and ε_r is the relative permittivity of the substrate used.

For further investigation of the band notch characteristics, the current vector distribution at 5.5 GHz, 8 GHz, and 10.5 GHz are shown inFigure 5(a)-(c), respectively. The maximum field strength was observed around the upper L-shaped slot, the lower L-shaped slot and the SRR, ensuring effective band rejection at 4.6-5.9 GHz, 8 GHz, and 10.5 GHz, respectively. Furthermore, The loading slot behaves like a half-wave resonator and becomes a closed-circuit at both ends. As a result, the input impedance becomes zero at the feed point, and the radiation in the notch band is reduced as shown in Figure 4. Also, as shown in the figure at 10.5 GHz the maximum amount of the power coupled with SRR and radiation of antenna diminished, since SRR is designed and placed both sides of the feed line to notch 10.5 GHz. The vector surface current distribution indicates that the proposed UWB MIMO antenna can efficiently reject the C-band, WLAN, and X-band.

[Figure 2 about here.]

3 Equivalent circuit of the half wavelength notch resonators

Figure 3 represents the equivalent circuit model of notched bands with lumped elements. It can be observed from three RLC resonators connected in parallel since the proposed

antenna has triple resonators with triple band notch characteristics. Also, shown in Figure 3, the first RLC resonator is designed to notch at 5.5 (4.6-5.9 GHz), the second RLC resonator designed notch at 8 GHz (7.70–8.43 GHz), and the third resonator designed at 10.5 GHz(10.3-10.98 GHz).

[Figure 3 about here.]

[Figure 4 about here.]

[Figure 5 about here.]

[Figure 6 about here.]

[Figure 7 about here.]

[Table 2 about here.]

4 Design procedures of the UWB MIMO antenna systems

We proposed a dual-port, dual-sided MIMO antenna configuration with triple-band notch characteristics, asFigure 7. As shown, the two-sided placement of the radiator and ground plane is introduced in the proposed MIMO antenna configuration. In the proposed method, the front side of the substrate consists of a polygon-shaped radiator(R1) and an inverted L-shaped ground (G2). Similarly, the backside of the substrate consists of a polygon-shaped shaped radiator(R2) and inverted L-shaped ground (G1). The double side placement of the radiator improves the isolation between the radiating elements compared to conventional radiator placement. In addition, since the two radiators are parallel to each other, pattern diversity is achieved, and isolation is improved.

4.1 Impact of the ground plane

The development of the inverted L-shaped ground plane is presented in Figure 6(a)-(c). An impedance matching achieved in the proposed MIMO antenna by using a partial ground plane. Also, the partial ground plane contributes to enhancing the isolation between the radiating elements by suppressing the surface current. Figure 6 shows the mutual coupling (S12, S21) of Antenna 1, Antenna 2, and Antenna 3 while feed 1 and feed 2 energized, respectively. Since Antenna 1(Figure 6(a)) has only a rectangular partial ground plane, it provides impedance matching and isolation, but isolation between

the radiating elements (S12 and S21 >- 5) is insufficient as shown in Figure 8. Similarly, S11/S22 for Antenna 1 indicated in Figure 9. It can be perceived from the Figure 9 Antenna 1 has impedance bandwidth of 4-12 GHz with a reflection coefficient of <-10dB except notch bands. Isolation and impedance bandwidth needs to be improved further for UWB MIMO application so, Antenna 2 (Figure 6 (b)) has a partial ground plane, and the ground plane is extruded vertically with a rectangular stub to improve isolation between radiating elements. The vertical stub is reducing mutual coupling by preventing the radiation, and it can be observed from Figure 8 and Figure 9 it provides greater than 14 dB (S12 & S21) isolation and impedance bandwidth of 3 -12 dB with S11<-10dB except 6-8 GHz, 9-9.6 GHz and notch bands, respectively. Therefore, isolation and impedance bandwidth is not sufficient for UWB MIMO antenna. Furthermore, Antenna 2 is modified by connecting the horizontal stub to the extruded vertical line, the isolation of the Antenna 3 (Figure 6(c)) is further improved since the vertical line, and horizontal line stubs suppress surface current distribution and mitigate the mutual coupling. Furthermore, in order to improve the impedance bandwidth at 6-8 GHz, and 9-9.6 GHz rectangular shaped slot removed in partial ground plane as shown in Figure 6(c). Because of the modifications the Antenna 3 improves bandwidth that is 3 -12 dB with S11/S22 of <-10dB except notch band as shown in Figure 9. In this case, the isolation is improved in the 3 to 12 GHz range. It is observed that from Figure 8 isolation greater than 19 dB is realized over the entire operating band, that is significantly lower and sufficient for MIMO performance.

[Figure 8 about here.]

To demonstrate the influence of the proposed inverted L-shaped stub decoupling structure in a proposed MIMO antenna, the surface current distribution at 3.3 GHz, 6.5 GHz, and 9 GHz when port 1/port 2 excited are depicted in Figure 10(a)-(d). As shown in Figure 10(a)-(d) at 3.3 GHz, 6.5 GHz, and 9 GHz, when port 1 is energized, there is no coupling current between polygon-shaped radiator R1 and R2, and port 2 is energized vice versa. In the presence of inverted L-shaped stub decoupling structure, the antenna surface current at the ground is reduced from 80.5 A/m to approximately 39.5 A / m, so as shown Figure 10 (a)-(d), the coupling current is reduced by more than 50%. Therefore, isolation improved that is greater than 20dB over the UWB range.

[Figure 9 about here.]

[Figure 10 about here.]

The proposed dimension of the antenna mentioned in Table 2. Furthermore, the overall dimension of the two-port MIMO antenna is only 28 x 18 mm^2, which is very small compared to existing two-port MIMO antennas, as mentioned in the Table 1. The proposed MIMO antenna is optimized and simulated in CST software. The optimized dimensions are used to fabricate on 1.6 mm thick FR4 substrates for measurements. The proposed MIMO antenna configuration front and back side is shown in Figure 7(a) and Figure 7(b). The proposed dimension of the antenna is given in Figure 7.

5 The performance analysis of the polygon-shaped UWB MIMO antenna

5.1 Simulation and measured S-parameters

The proposed MIMO antenna is fabricated on FR4 substrate and measured by using keysight technologies N9926A vector network analyzer to validate the simulation results. Photograph of a fabricated antenna and VNA measurement shown in Figure 12. Figure 11 shows the comparison of simulated and measured reflection coefficients (S11/S22). It is perceived that the proposed MIMO antenna has impedance bandwidth from 3-12 GHz with reflection coefficient (S11/S22) of <-10 dB except for the notch bands. Furthermore, it can be observed from measured results (S11/S22) it has greater than -5 dB reflection coefficients at 4.6-4.9 GHz, 5-5.9 GHz, 8 GHz and 10.5 GHz since at this notch band frequency radiation suppressed by half-wave length notch inverted L-shaped slot resonators and SRR. It can be observed from the comparison results there is small mismatch between simulated and measured due to manufacturing error, soldering and loss at SMA connector. However, it has acceptable matching between simulated and measured results.Figure 13, shows the comparison of simulated and measured S12/S21 of the proposed MIMO antenna. The measured results show that the isolation(S12/S21) of proposed MIMO antenna with double side inverted L-shaped decoupling structure is greater than 19 dB over the 3-12 GHz between polygon-shaped radiator. It is perceived that simulated and measured results are approximately identical. Hence, the proposed UWB MIMO antenna is appropriate for short range communication applications.

[Figure 11 about here.]

[Figure 12 about here.]

[Figure 13 about here.]

5.2 VSWR of proposed triple notch UWB MIMO antenna

The proposed UWB MIMO antenna operates over 3-12 GHz while notching the satellite C band(4.6-4.9 GHz), WLAN (5–5.9 GHz), and the uplink and downlink of X-band satellite communication (7.70–8.43 GHz and 10.5–11 GHz) frequency bands. Typically, the VSWR of the antenna should be less than 2 throughout the operating band. Initially, the Radiator 1 has an impedance bandwidth of 3-12 GHz without notch band characteristics. So, it can be observed from Figure 14 that the proposed antenna has a VSWR of less than 2 from 3-12 GHz. From Figure 14 it can be observed that Radiator 2 has greater than 2 VSWR due to band notch at satellite C band(4.6-4.9 GHz) and WLAN (5–5.9 GHz) frequency bands. VSWR of Radiator 3 perceived form Figure 14, it has VSWR of greater than 2 at satellite C band(4.6-4,9 GHz), WLAN (5–5.9 GHz) and the uplink of X-band

satellite communication (10.3-10.98 GHz) due to notch characteristics. In the case of the proposed UWB MIMO antenna (Radiator 4) with notch band characteristics the VSWR at C band(4.6-4.9 GHz), WLAN (5–5.9 GHz) GHz, the uplink and downlink of X-band satellite communication (7.70–8.43 GHz and 10.3-10.98 GHz) frequency bands, it has VSWR of greater than 2 as shown in Figure 14. From a comparison of simulated VSWR, it is clear that the proposed MIMO antenna has a triple-band notch characteristics.

[Figure 14 about here.]

[Figure 15 about here.]

6 Radiation characteristics

The simulated and measured 2D radiation patterns of the proposed antenna gain in the E-plane and H-plane plane at 3.2, 6.5, 8 GHz and 9 GHz are shown in Figure 15(a) - (d). As can be seen from the radiation pattern, the maximum gain in the 235 ° direction at 3.2 GHz is 2.2 dB, and the gain in the 129 ° direction at 9 GHz is 6 dB while feed 1 (port 1) excited. Similarly, the maximum gain in the 285 ° direction at 3.2 GHz is 3 dB, and the gain in the 200 ° direction at 9 GHz is 7 dB while port 2 excited. It can be observed from the comparison results there is small mismatch between simulated and measured due to manufacturing error, soldering and loss at SMA connector. Finally, it can be seen in Figure 15 (a) -(d) that the proposed MIMO antenna has an almost omnidirectinal radiation pattern throughout the operating UWB frequency band.

6.1 Gain of proposed antenna

Figure 16 shows the comparison of simulated and measured peak gain of the proposed MIMO antenna with a triple notch band characteristics. The gain of MIMO antenna measured while port 1 is energized, and port 2 is closed. As can be seen from Figure 16, the realized peak gain varies between 0-7.5 dB, but at notch frequency band, the gain is greatly suppressed. In addition to that the gain of the antenna at 5 GHz(4.6-5.9 GHz), 8 GHz (7.79-8.43GHz), and 10.5 GHz(10.3-10.98 GHz), is -5 dB, -2 dB and -2 dB, respectively. It is evident from the Figure 16, the proposed antenna is suitable for UWB MIMO applications with notch characteristics.

[Figure 16 about here.]

6.2 Simulated and measured antenna efficiency

Figure 17 shows the comparison of simulated and measured efficiency of the proposed MIMO antenna with a triple notch characteristics. The efficiency of MIMO antenna measured while port 1 is energized, and port 2 is closed. It is perceived that from Figure 17, the efficiency of UWB MIMO antenna 85 % over 3-12 GHz , but at notch frequency

band, the gain is efficiency reduced. In addition to that the efficiency of the antenna at 5.5 GHz(4.6-5.9 GHz), 8 GHz (7.79-8.43 GHz), and 10.5 GHz (10.3-10.98 GHz), is less than 40 %. It can be observed that the proposed antenna is suitable for UWB MIMO applications with notch characteristics.

[Figure 17 about here.]

7 MIMO performance

7.1 Envelope correlation coefficient (ECC) and diversity gain (DG)

The ECC and DG are essential metrics to assess the MIMO performance of the proposed antenna. The correlation between radiating elements can be analyzed based on ECC. Using the S-parameters and the 2D radiation pattern, calculate the ECC with the following formula:

$$ECC = \frac{\left|\iint[\overrightarrow{S}_a(\theta,\phi).\overrightarrow{S}_b(\theta,\phi)]\,d\Omega\right|^2}{\iint\left|[\overrightarrow{S}_a(\theta,\phi)]\right|^2 d\Omega \iint\left|\overrightarrow{S}_b(\theta,\phi)]\right|^2 d\Omega} \tag{5}$$

$$ECC = \frac{\left|\iint[\overrightarrow{S}_a(\theta,\phi).\overrightarrow{S}_b(\theta,\phi)]\,d\Omega\right|^2}{\iint\left|[\overrightarrow{S}_a(\theta,\phi)]\right|^2 d\Omega \iint\left|\overrightarrow{S}_b(\theta,\phi)]\right|^2 d\Omega} \tag{6}$$

[Figure 18 about here.]

The ECC of the completely decoupled radiating element is zero, but for practical conditions, the ECC value can be <0.5. The simulated and measured ECC for the proposed antenna with double side inverted L-shaped ground is presented in the Figure 18. As can be seen from the Figure 18, over the 3-12 GHz band, the ECC values are 0.002 and 0.0025, respectively, for simulated and measured. Furthermore, it is clear that the correlation between the radiators is very low. The following equation can be used to estimate the Diversity Gain (DG) of the proposed double side MIMO antenna

$$\mathrm{DG} = 10\sqrt{1 - \mathrm{ECC}^2}. \tag{7}$$

The simulated diversity gain of the antenna is shown inFigure 19. As can be seen from the figure, DG > 9.9 for the entire operating band.

[Figure 19 about here.]

7.2 Multiplexing efficiency

Multiplexing efficiency is an advantageous metric to optimize channel capacity, address the imbalance between antenna efficiency and correlation. It can be observed from Figure 20, the multiplexing efficiency of antenna 85 % over UWB MIMO antenna, but at notch frequency band the multiplexing efficiency reduced. In addition to that the multiplexing efficiency of the antenna at 4.6-5.9 GHz, 8 GHz, and 10.5 GHz, is less than 40 %

$$\eta_{\mathrm{MUX}} = \sqrt{(1 - |\rho_c|^2)\eta_1\eta_2} \tag{8}$$

[Figure 20 about here.]

[Figure 21 about here.]

7.3 Total Active Refection Coefficients(TARC)

When simultaneously stimulating adjacent elements of a MIMO antenna, TARC is one of the significant parameters for predicting the performance of a MIMO system. Since the S-parameter is only insufficient to analyze the performance of the MIMO antenna performance. TARC can be calculated by the following formula.

$$\text{TARC} = \sqrt{\frac{(S_{11} + S_{12})^2 + (S_{21} + S_{22})^2}{2}} \tag{9}$$

The efficient MIMO antenna system should have < 0 dB of TARC value. It can be perceived from Figure 21 the proposed UWB MIMO has TARC value of less than -10 dB from 3-12 GHz.

7.4 Channel capacity loss(CCL)

In MIMO antenna system channel capacity loss(CCL) indicating the effect of the correlation between the radiating elements. The allowable channel capacity loose (CCL) for MIMO antenna systems is less than 0.5 bits / Hz / second[22]. CCL can be estimated from S-parameters of the MIMO antenna by using the following equations

$$C(Loss) = -\log_2 \ det(\psi^R) \tag{10}$$

$$\psi^R = \begin{bmatrix} \rho_{11} & \rho_{12} \\ \rho_{21} & \rho_{22} \end{bmatrix} \tag{11}$$

Where

$$\rho_{aa} = 1 - \left(|S_{aa}|^2 + |S_{ab}|^2\right) \tag{12}$$

$$\rho_{ab} = -\left(S^*_{aa}S_{ab} + S^*_{ba}S_{ab}\right) \ for \ a, \ b \ = 1 \ or \ 2 \tag{13}$$

[Figure 22 about here.]

As can be perceived from Figure 22 the CCL of the proposed MIMO antenna is less than 0.5 bits/Hz/s. Hence, the proposed antenna suitable for MIMO applications.

8 Comparison of the proposed antenna with other cutting-edge designs

The proposed UWB MIMO antenna and recently published UWB MIMO antenna comparison presented in Table 1. It can be observed from Table 1 proposed UWB MIMO antenna is beneficial in terms of triple notched bands with double side radiator placement, compact size, and improved isolation.

9 Validation of proposed UWB MIMO using Universal Software Radio Peripheral(USRP)

The real-time short-range communication performance analysis of the proposed UWB MIMO antenna experimentally investigated using indoor base stations. The experiment set up consist of two base stations(base stion1 and the base station 2). Each base station consists of NI USRP, proposed MIMO antenna, and 802.11 frameworks. As a performance evaluation metric, the received power and throughput speed considered. Two proposed UWB MIMO antennas are connected with two USRP's then video signal is transmitted and received through it. In addition to that, short-range communication performance analysis was done with different cases, as shown in Table 3. Figure 23, shows the block diagram of an indoor base station based video transmission and reception using NI USRP 2943R and proposed MIMO antenna.

[Figure 23 about here.]

[Figure 24 about here.]

[Table 3 about here.]

The base station 1 includes a proposed 2-port MIMO antenna 1 having radiating elements A, B. Similarly, the base station 2 includes a proposed 2-port MIMO antenna 2 with radiating elements C, D. Two different cases realized to validate the MIMO antenna real-time performance for short-range wireless transmission as follows, in Case1: Antennas A and B are considered transmitters and antennas C and D are considered receivers. Similarly, Case 2: ReAntennas B, D are considered transmitters and antennas A, C are considered receivers.
Figure 24 displays the indoor base station based measurement setup of the proposed MIMO antenna. In addition, the proposed MIMO antenna is located at a different distance, such as 1 m, 1.5 m, and 2 m. Figure 24 displays the indoor base station based measurement setup of the proposed MIMO antenna at a different distance. It can be perceived from the Table 3, RSRP results with the two cases using the proposed MIMO antenna are <-40 dBm (Case 1), and <-40 dBm(Case 2). Furthermore, throughput speed for case 1 using the proposed UWB MIMO antenna is 2 Mb/s, 1.5 Mb/s, and 1 Mb/s at 1, 1.5 and 2 m respectively. Likewise, throughput speed for case 2 using the proposed UWB MIMO antenna is 2 Mb/s, 1.5 Mb/s, and 1 Mb/s at 1, 1.5 and 2 m respectively. Hence, the proposed four UWB MIMO antennas appropriate to operate as a transmitter /receiver due to its identical performance and is appropriate for real-time short-range communication applications.

10 Conclusion

The highly isolated double side triple band notched UWB MIMO antenna for short range communication applications is proposed and studied experimentally. The double placement of radiator and inverted L-shaped ground is implemented with compact size of 18 $\times$

$28mm^2$. The proposed antenna designed to operate at UWB band(3-12 GHz) with notched band at IEEE INSAT C band satellite communication (4.6-4.9 GHz), WLAN band (5–5.9 GHz), and the X band up link and down link satellite communication (7.70–8.43 GHz and 10.3-10.98 GHz). The high isolation is realized by double side placement and extruding inverted L-shaped decoupling stub on the partial ground plane. An Isolation between the two radiators is >19 dB over 3–12 GHz, and obtained gain is 0–7.5 dBi over operating band. The proposed UWB MIMO antenna has a very low ECC of 0.0025 and a diversity gain >9.98 dB across the entire operating band. The real-time short range transmission and reception also demonstrated using NI USRP to prove the performance of the fabricated antenna. The proposed antenna has good consistency in the simulation and measurement results, and real-time demonstration showed that proposed UWB MIMO antenna appropriate for short range wireless communication applications.

References

[1] V. P. T. A. Sibille, ‘"Spatial multiplexing in UWB MIMO communications," ’,Electronics Letters, 2006, pp. 931–932.

[2] Revision of part 15 of the commissions rules regarding ultra-wide-band transmission systems first report and order";2002.

[3] J. Naveen, D. G. Samir, and T. Ekta, Triple band notched mushroom and uniplanar EBG structures based UWB MIMO/Diversity antenna with enhanced wide band isolation, AEU - International Journal of Electronics and Communications (2018).

[4] Fractal EBG structure for shielding and reducing the mutual coupling in microstrip patch antenna array’, AEU - International Journal of Electronics and Communications (2018).

[5] A. Iqbal, O. A. Saraereh, and A. W. Ahmad, Mutual Coupling Reduction Using F-Shaped Stubs in UWB-MIMO Antenna, IEEE Access (2018), 2755–2759.

[6] R. C, A. KG, and K. R, Tapered Fed Compact UWB MIMO-Diversity Antenna With Dual Band-Notched Characteristics, IEEE Transactions on Antennas and wave propagation (2018), April;66(4):1677–1684. Available from: 10.1109/TAP.2018.2803134.

[7] C. N. Pratima, N. Anil, and N. Sanjay, Compact wideband MIMO antenna for 4G WI-MAX, WLAN and UWB applications, AEU -International Journal of Electronics and Communications (2019).

[8] KaushikMandal JuinAcharjee and undefined KumarMandal, Reduction of mutual coupling and cross-polarization of a MIMO/diversity antenna using a string of H-shaped DGS, AEU - International Journal of Electronics and Communications 97 (2018), 110–119.

[9] Rifaqat Hussain, Mohammad S. Sharawi, Atif Shamim, et al., An Integrated Four-Element Slot-Based MIMO and a UWB Sensing Antenna System for CR Platforms, IEEE Transactions on Antennas and Propagation 66 (2018), no. 2, 978–983.

[10] Zhijun Tang, Xiaofeng Wu, Jie Zhan, Shigang Hu, Zaifang Xi, and Yunxin Liu, Design of ultra-compact UWB antenna with band-notched characteristics for MIMO applications, IET Microwaves, Antennas & Propagation 12 (2018), no. 12.

[11] A. A. R. Saad, Approach for improving inter-element isolation of orthogonally polarised MIMO slot antenna over ultra-wide bandwidth, Electronics Letters.2018;54(18):1062–1064. Available from:, 10–1049.

[12] B. Niu and J. Tan, Compact SIW cavity MIMO antenna with enhanced bandwidth and high isolation, Electronics Letters 55(11) (2019), 631–632.

[13] R. Chandel and A. K. G. K. Rambabu, Design and Packaging of an Eye-Shaped Multiple-Input–Multiple-Output Antenna With High Isolation for Wireless UWB Applications, IEEE Transactions on Components, Packaging and Manufacturing Technology (2018).

[14] P. Palanisamy and Subramani M, Novel Double-Side EBG Based Mutual Coupling Reduction for Compact Quad Port UWB MIMO Antenna, AEU - International Journal of Electronics and Communications (2019).

[15] A compact double-sided MIMO antenna with an improved isolation for UWB applications, International Journal of Electronics and Communications (AEÜ) 82 (2017), 7–13.

[16] Z. Li, C. Yin, and X. Zhu, Compact UWB MIMO Vivaldi Antenna With Dual Band-Notched Characteristics, IEEE Access 7 (2019), 38696–38701.

[17] Z. Tang, X. Wu, J. Zhan, S. Hu, Z. Xi, and Y. Liu, Compact UWB-MIMO Antenna With High Isolation and Triple Band-Notched Characteristics, IEEE Access 7 (2019), 19856–19865.

[18] M. Shehata, M. S. Said, and H. Mostafa, Dual Notched Band Quad-Element MIMO Antenna With Multitone Interference Suppression for IR-UWB Wireless Applications, IEEE Transactions on Antennas and Propagation 66 (2018), no. 11, 5737–5746.

[19] A.S. Abd El-Hameed, M. G. Wahab, Ayman Elboushi, and Marwa S. Elpeltagy, Miniaturized triple band-notched quasi-self complementary fractal antenna with improved characteristics for UWB applications, AEU - International Journal of Electronics and Communications 108 (2019), 163–171.

[20] Soufian Lakrit, Sudipta Das, Ali El Alami, Debaprasad Barad, and Sraddhanjali Mohapatra, A compact UWB monopole patch antenna with reconfigurable Band-notched characteristics for Wi-MAX and WLAN applications, AEU - International Journal of Electronics and Communications 105 (2019), 106–115.

[21] Amir H. Nazeri, A. Falahati, and R. M. Edwards, A novel compact fractal UWB antenna with triple reconfigurable notch reject bands applications, AEU - International Journal of Electronics and Communications 101 (2019), 1–8.

[22] Kunal Srivastava, Binod Kumar Kanaujia, Santanu Dwari, Sachin Kumar, and Taimoor Khan, 3D cuboidal design MIMO/diversity antenna with band notched characteristics, AEU - International Journal of Electronics and Communications 108 (2019), 141–147.

[23] Irene Suriya and Rajesh Anbazhagan, Inverted-A based UWB MIMO antenna with triple-band notch and improved isolation for WBAN applications, AEU - International Journal of Electronics and Communications 99 (2019), 25–33.

[24] José Alfredo Tirado-Méndez, Ricardo Gómez-Villanueva, Hildeberto Jardón-Aguilar, Erik Fritz-Andrade, and Arturo Rangel-Merino, UWB MIMO antenna implemented with orthogonal quasi-circular slot dipole radiators, International Journal of RF and Microwave Computer-Aided Engineering 0, no. 0, e21974.

[25] Rakesh N. Tiwari, Prabhakar Singh, and Binod K. Kanaujia, A compact UWB MIMO antenna with neutralization line for WLAN/ISM/mobile applications, International Journal of RF and Microwave Computer-Aided Engineering 29 (2019), no. 11, e21907.

[26] K Vasu Babu and Bhuma Anuradha, Design of MIMO antenna to interference inherent for ultra wide band systems using defected ground structure, Microwave and Optical Technology Letters 61 (2019), no. 12, 2698–2708.

[27] Ming-Tao Tan, Xiang Li, Wang-He Wei, Wen-Xue Tan, Bin Zhou, and Jian-Qi Li, A planar miniaturized UWB dual-polarization multiple-input-multiple-output slot antenna, Microwave and Optical Technology Letters 0, no. 0.

[28] Sachin Kumar, Gwan H. Lee, Dong H. Kim, Wahab Mohyuddin, Hyun C. Choi, and Kang W. Kim, Multiple-input-multiple-output/diversity antenna with dual band-notched characteristics for ultra-wideband applications, Microwave and Optical Technology Letters 0, no. 0.

[29] Narinder Sharma and Sumeet S. Bhatia, Design of printed monopole antenna with band notch characteristics for ultra-wideband applications, International Journal of RF and Microwave Computer-Aided Engineering 29 (2019), no. 10, e21894.

[30] Anil K. Gautam, Anjali Saini, Niraj Agrawal, and Navaid Z. Rizvi, Design of a compact protrudent-shaped ultra-wideband multiple-input-multiple-output/diversity antenna with band-rejection capability, International Journal of RF and Microwave Computer-Aided Engineering 29 (2019), no. 9, e21829.

List of Figures

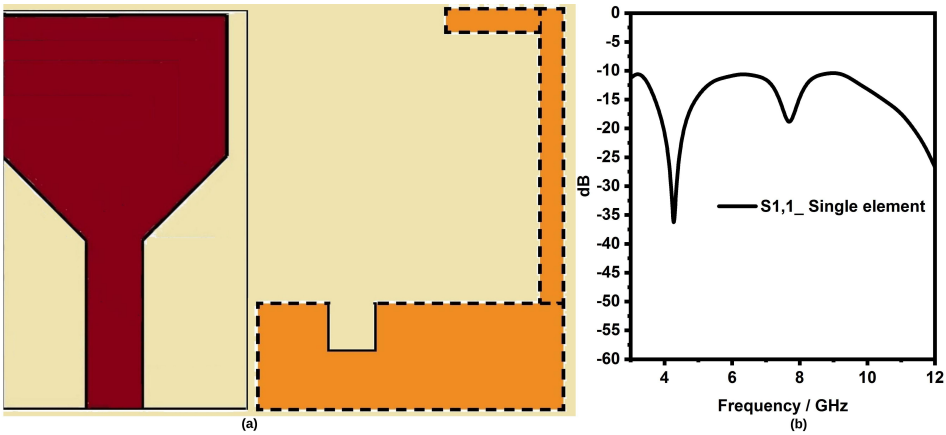

FIGURE 1: (a) Geometry of the proposed single element monopole antenna, (b) Reflection coefficients of single element.

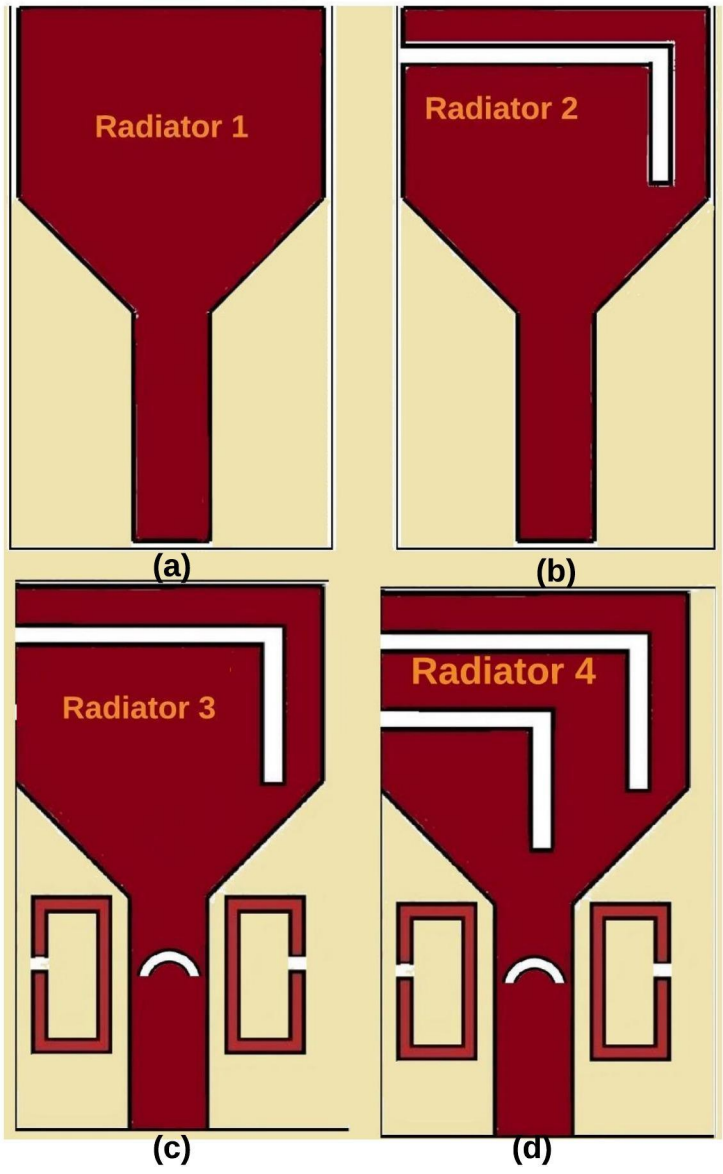

FIGURE 2: Development of proposed radiator, (a) Radiator 1, (b) Radiator 2, (c) Radiator 3 and (d) Radiator 4.

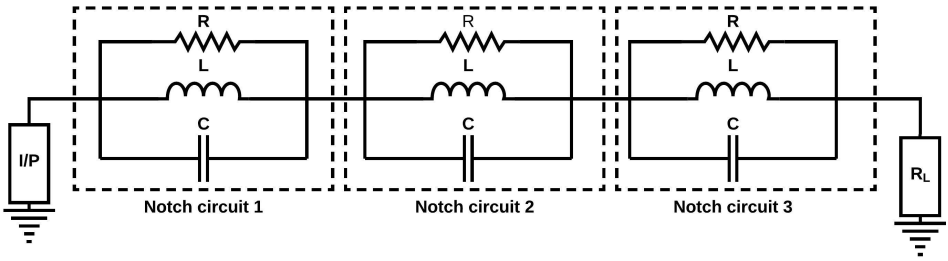

FIGURE 3: Lumped element equivalent circuit of half wave length notch resonators.

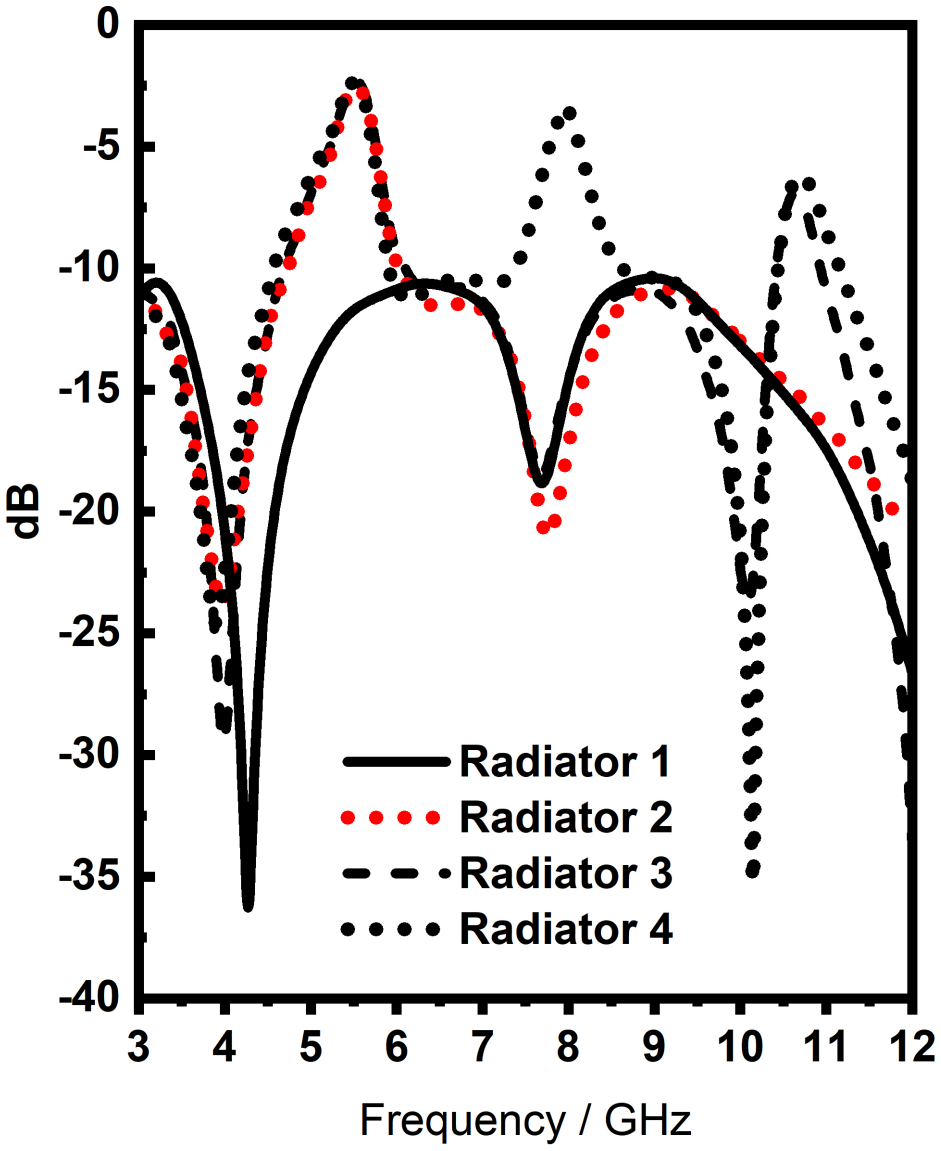

FIGURE 4: Reflection coefficients(S11/S22) of different radiators.

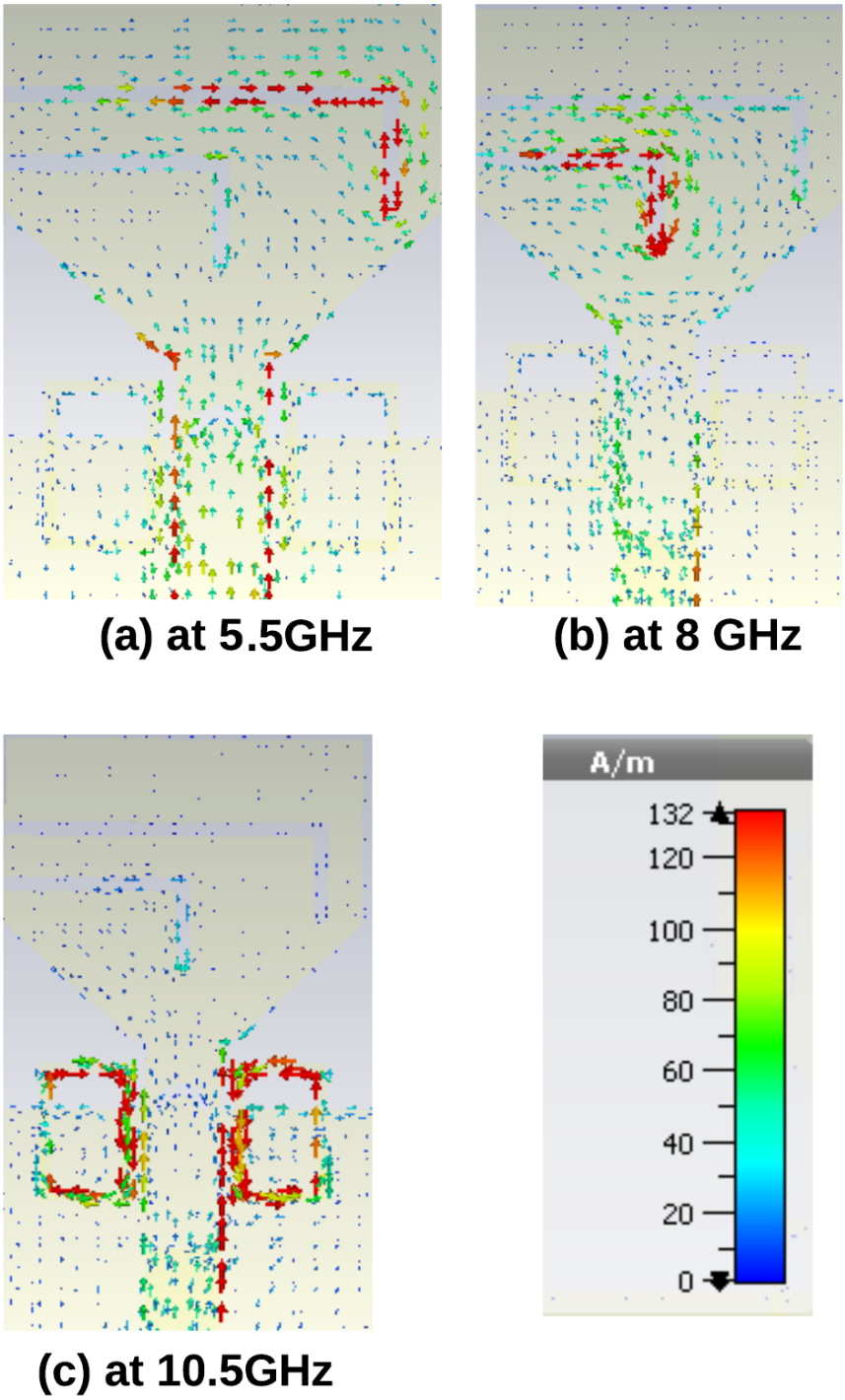

FIGURE 5: Vector current distribution of propose MIMO antenna (a) at 5.5 GHz, (b) at 8 GHz and (c) at 10.5 GHz

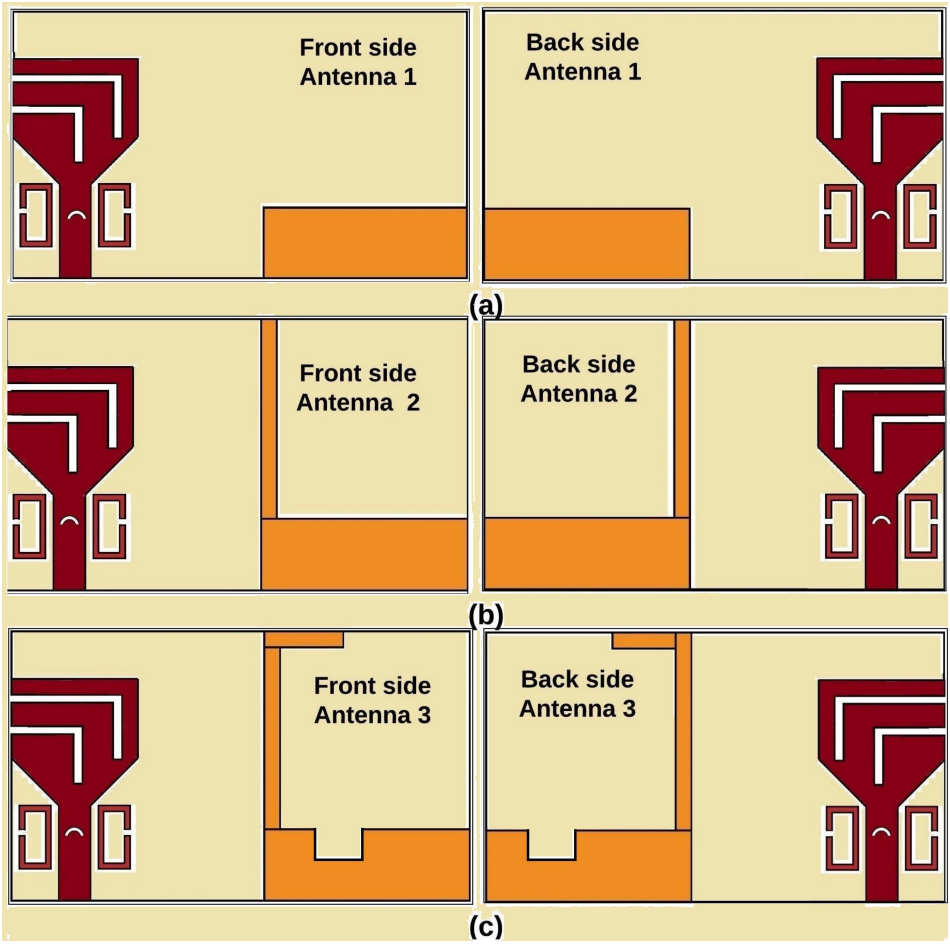

FIGURE 6: Development of ground structure for proposed MIMO antenna.(a) Antenna 1, (b) Antenna 2 and (c) Antenna 3.

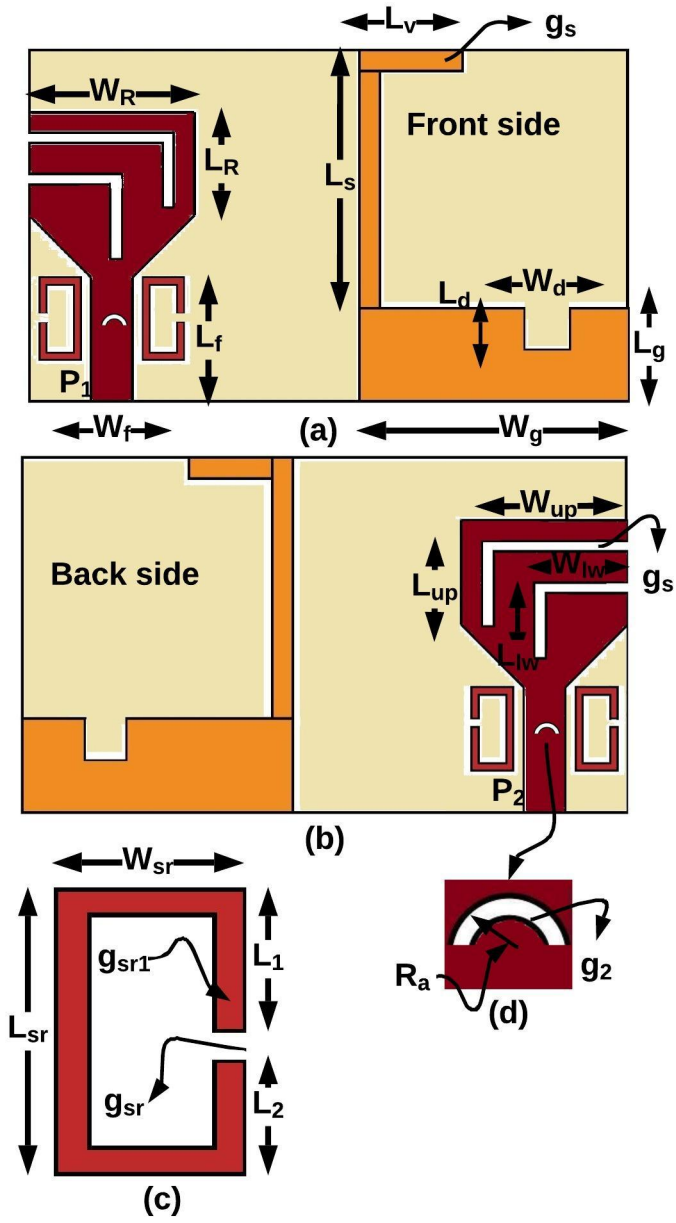

FIGURE 7: Structure of Proposed MIMO antenna (a) Front side, (b) Back side of proposed MIMO antenna, (c) Geometry of SRR , and (d) Geometry of semicircle

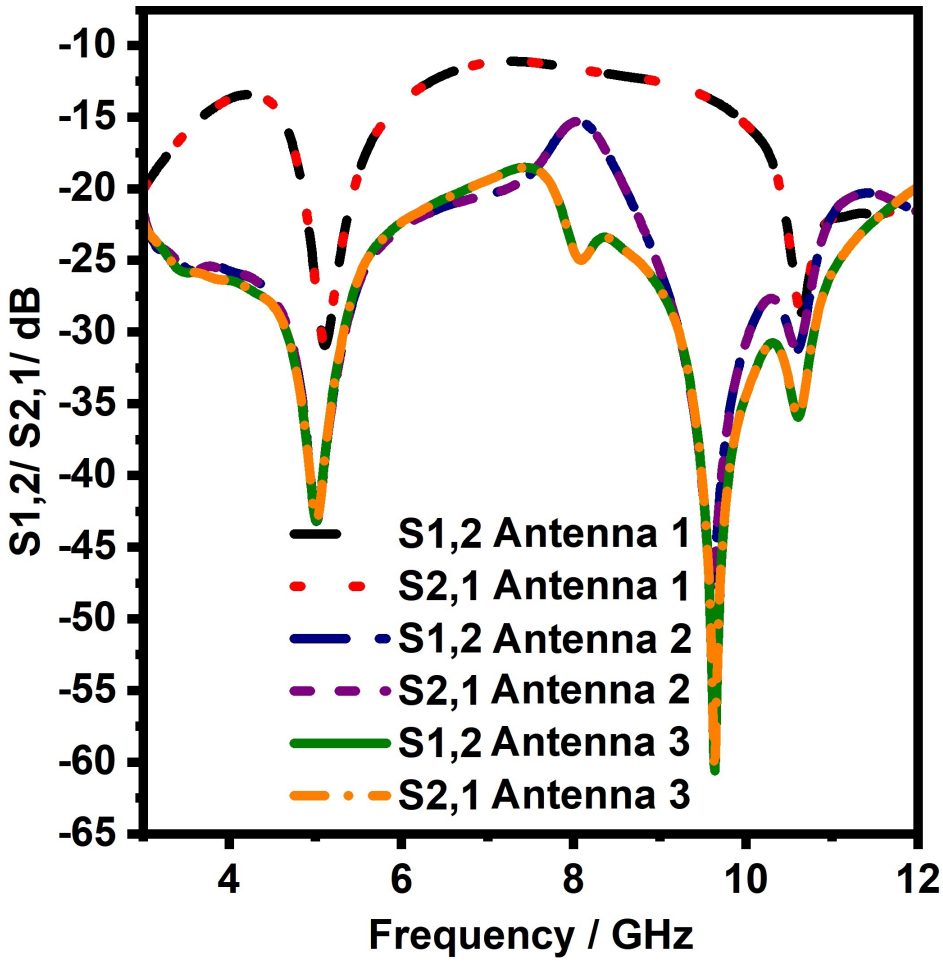

FIGURE 8: Isolation (S12/S21) of the different ground plane (Antenna 1, Antenna 2, and Antenna 3)

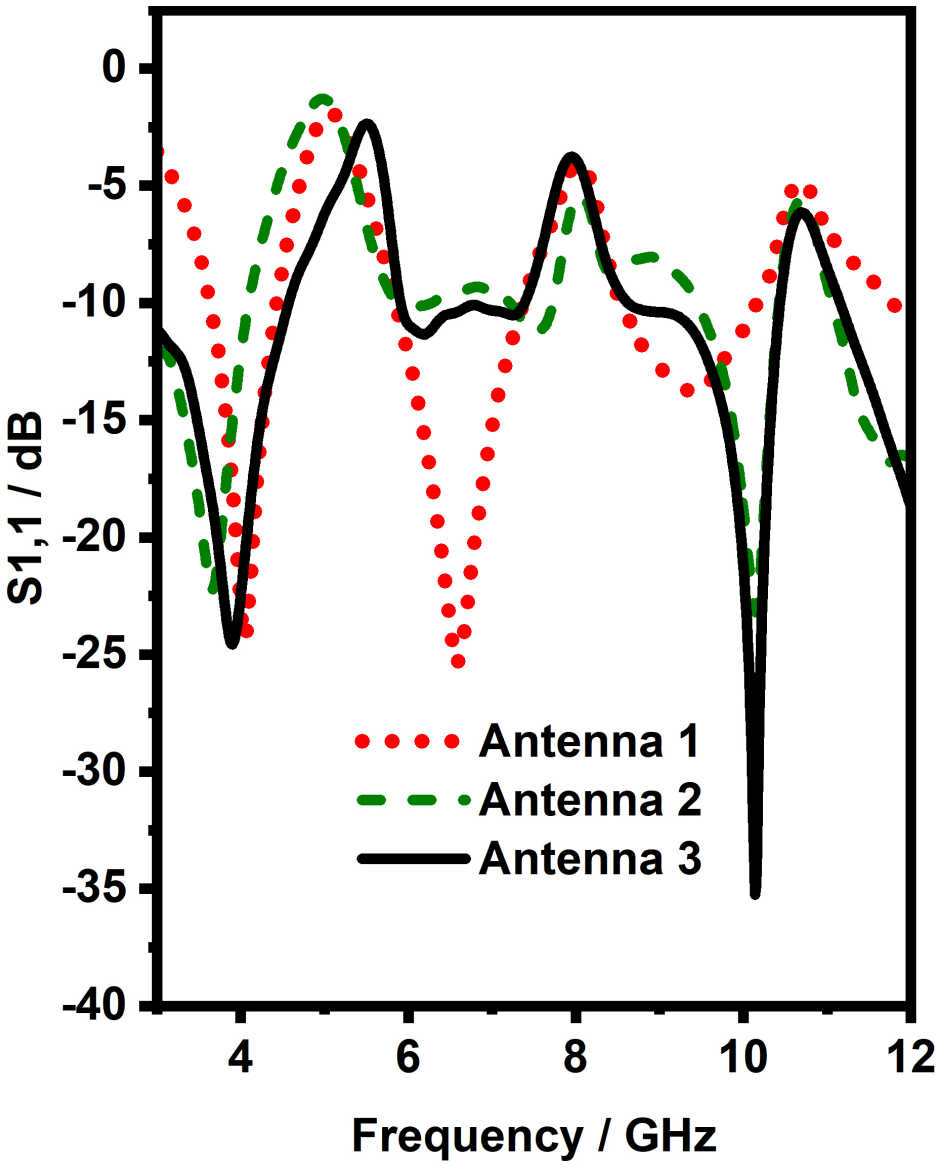

FIGURE 9: Simulated S11/ S22 of the proposed MIMO antenna for different ground structures(Antenna 1, Antenna 2, and Antenna 3)

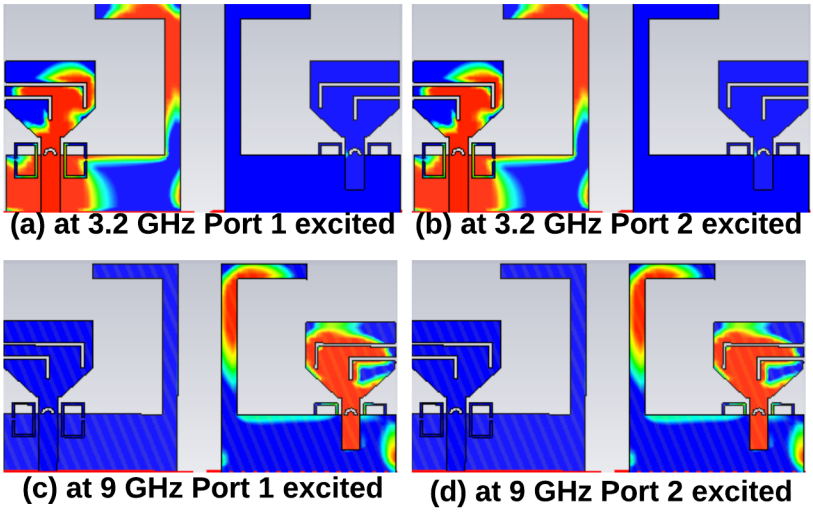

FIGURE 10: Surface current distribution of the MIMO antenna with inverted L shaped stub decoupling structure at 3.2 GHz and 9 GHz.

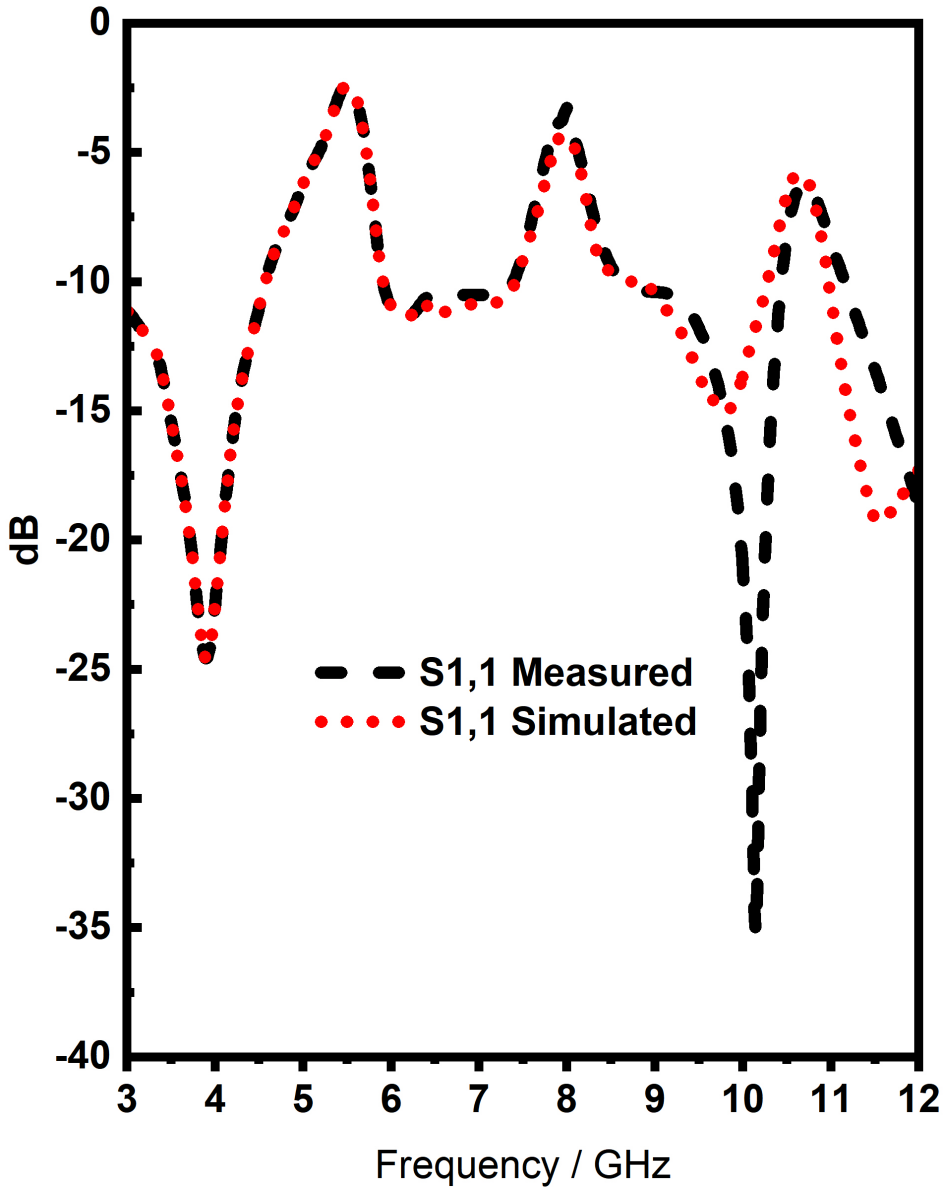

FIGURE 11: Comparison of simulated and measured S11/S22 of proposed MIMO antenna

FIGURE 12: Fabricated UWB MIMO antenna and measurement setup

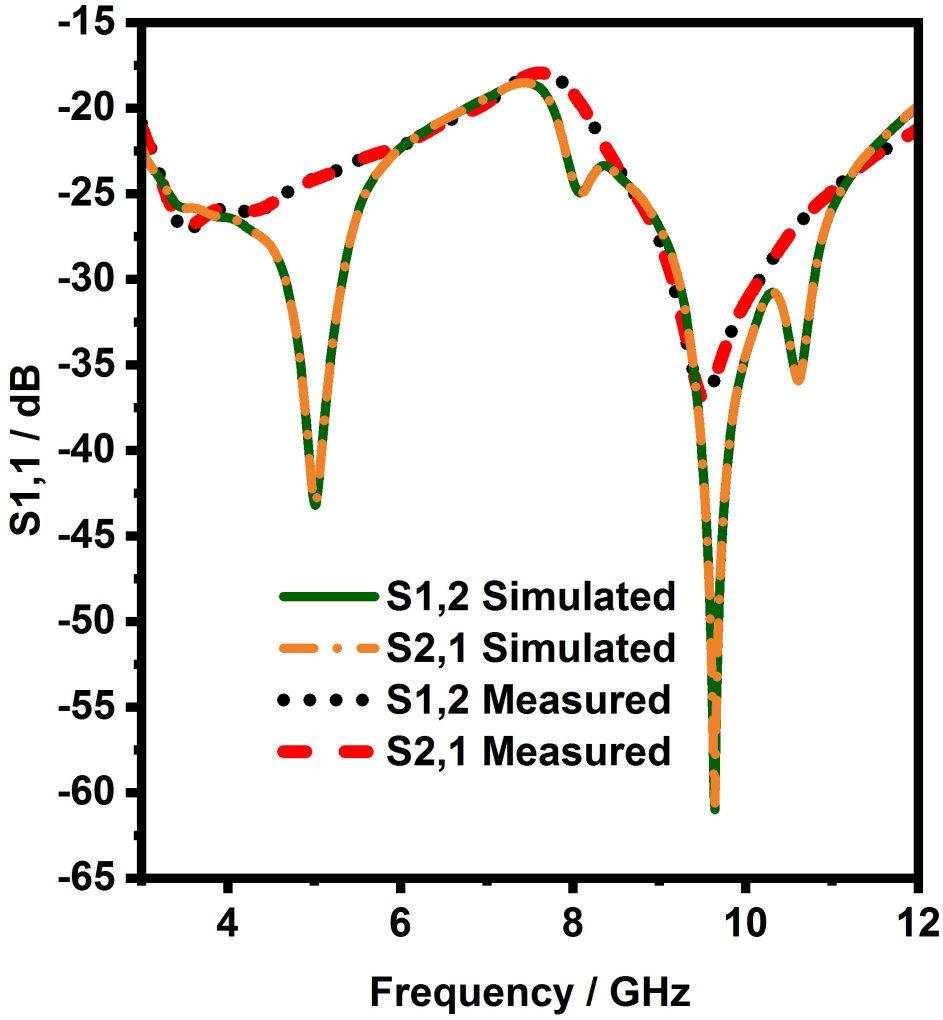

FIGURE 13: Simulated and measured mutual coupling (S12/S21) of proposed MIMO antenna

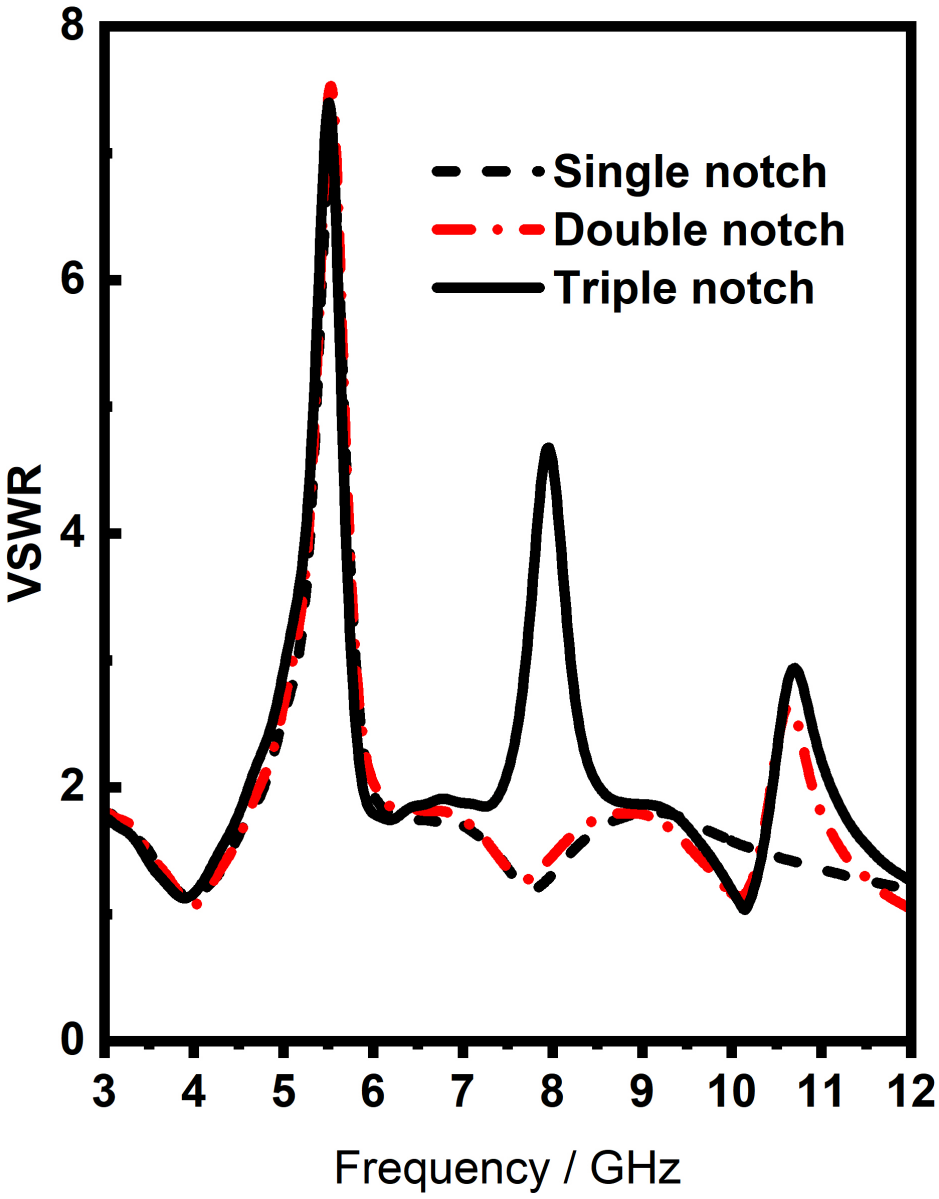

FIGURE 14: VSWR of proposed MIMO antenna for different radiator

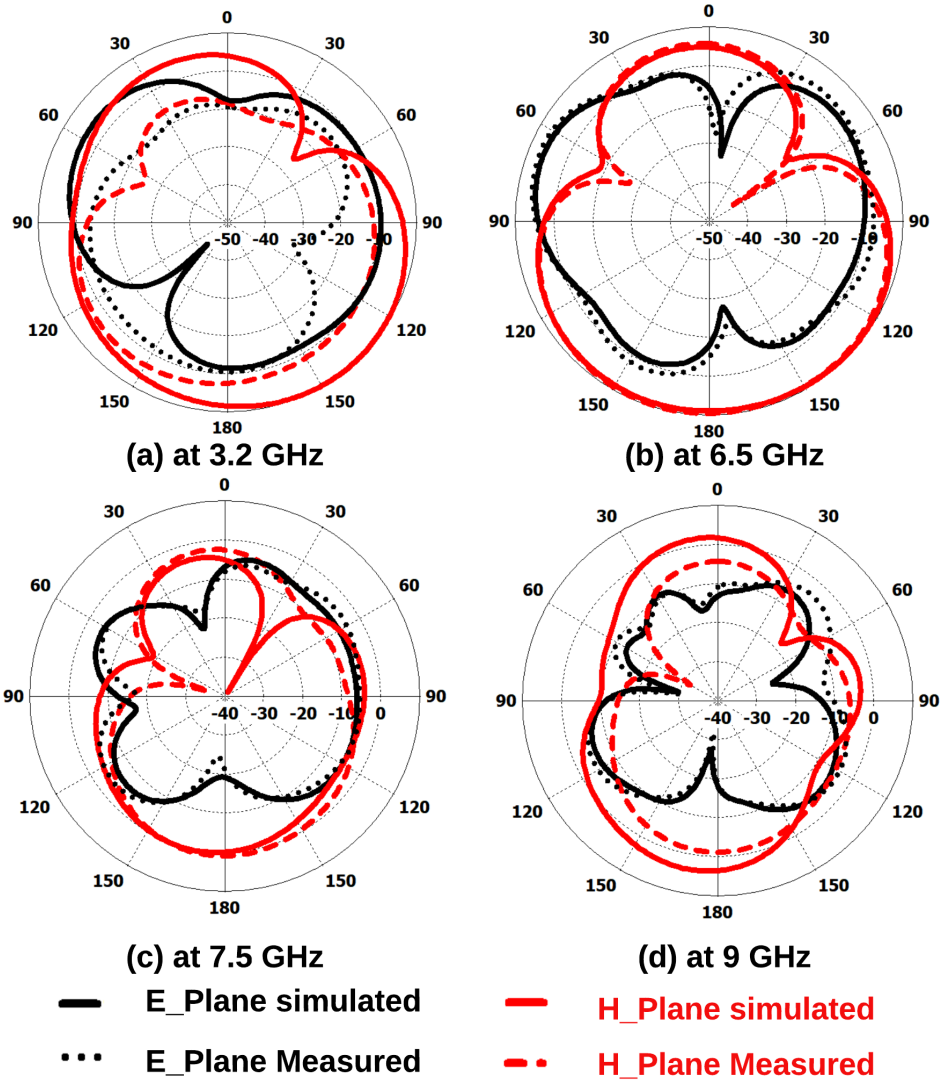

FIGURE 15: Simulated and measured radiation pattern (E-plane and H-plane) of the proposed antenna at 3.2 GH, 6.5 GHz, 7.5 GHz and 9 GHz

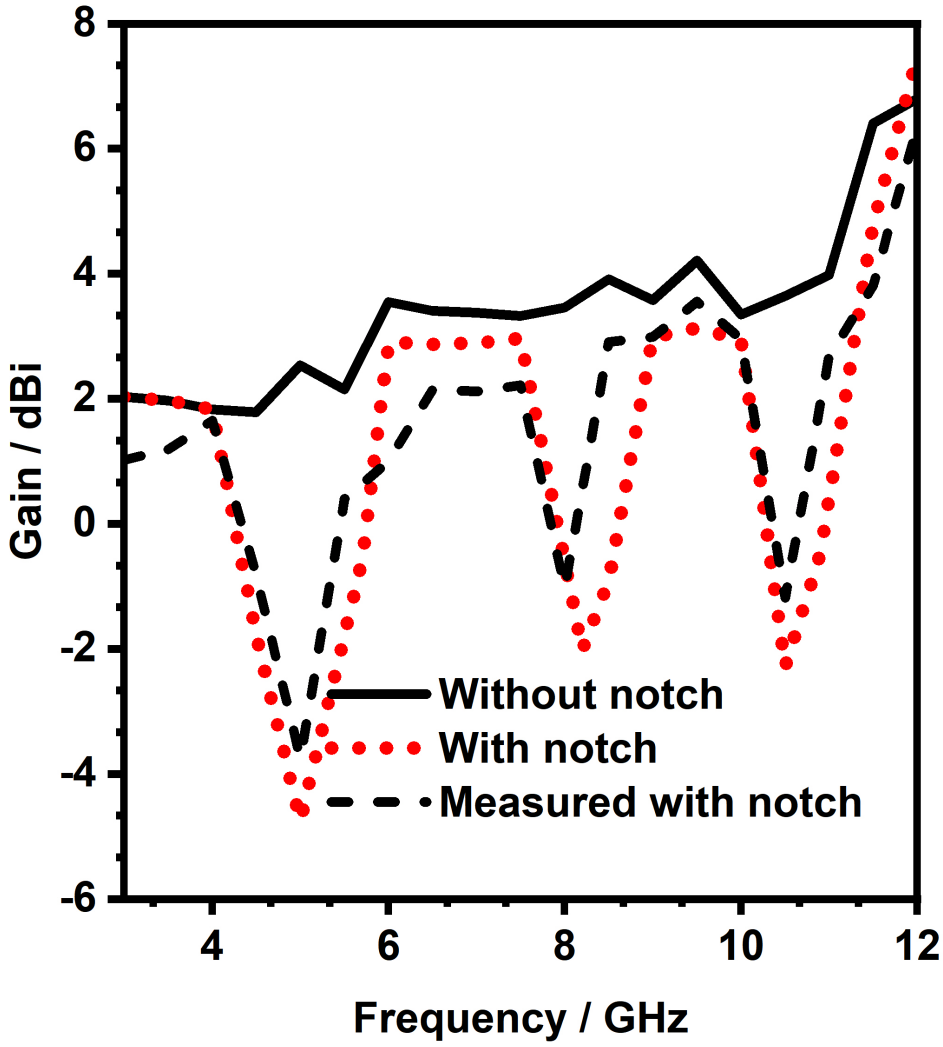

FIGURE 16: Gain of the proposed UWB MIMO antenna with notch characteristics

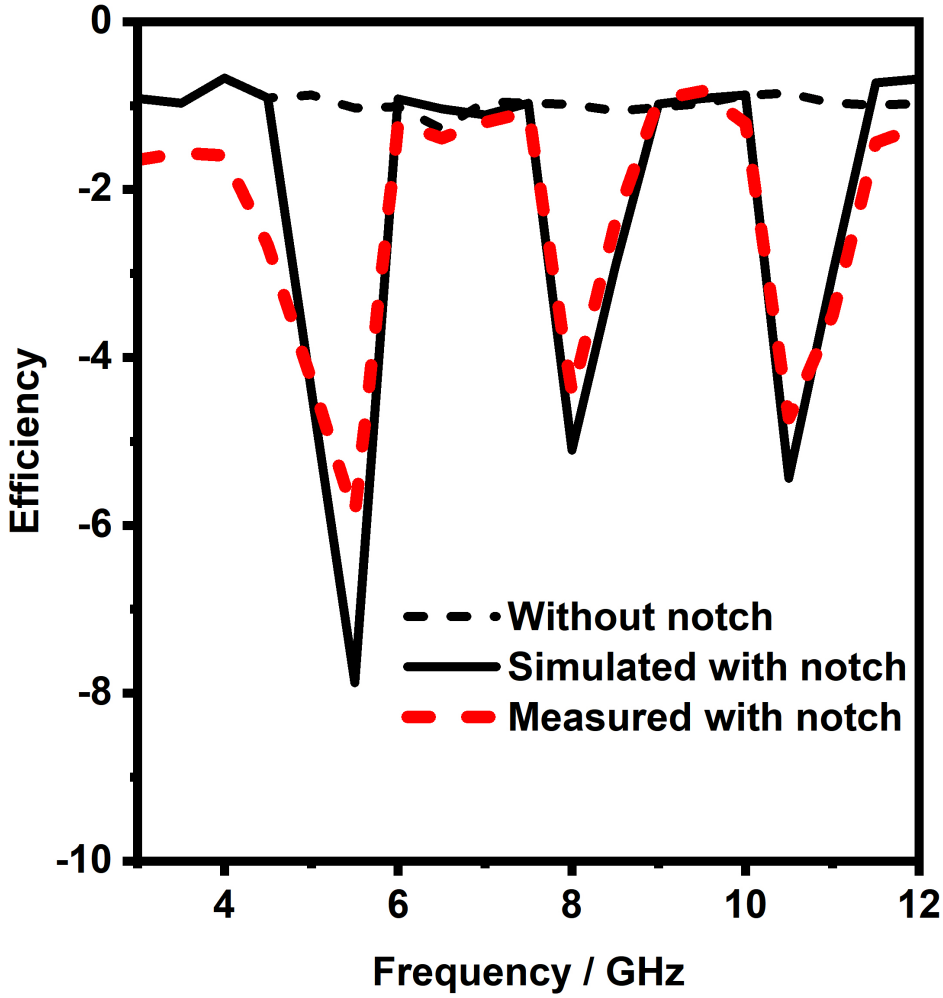

FIGURE 17: Efficiency of the proposed UWB MIMO antenna with notch characteristics

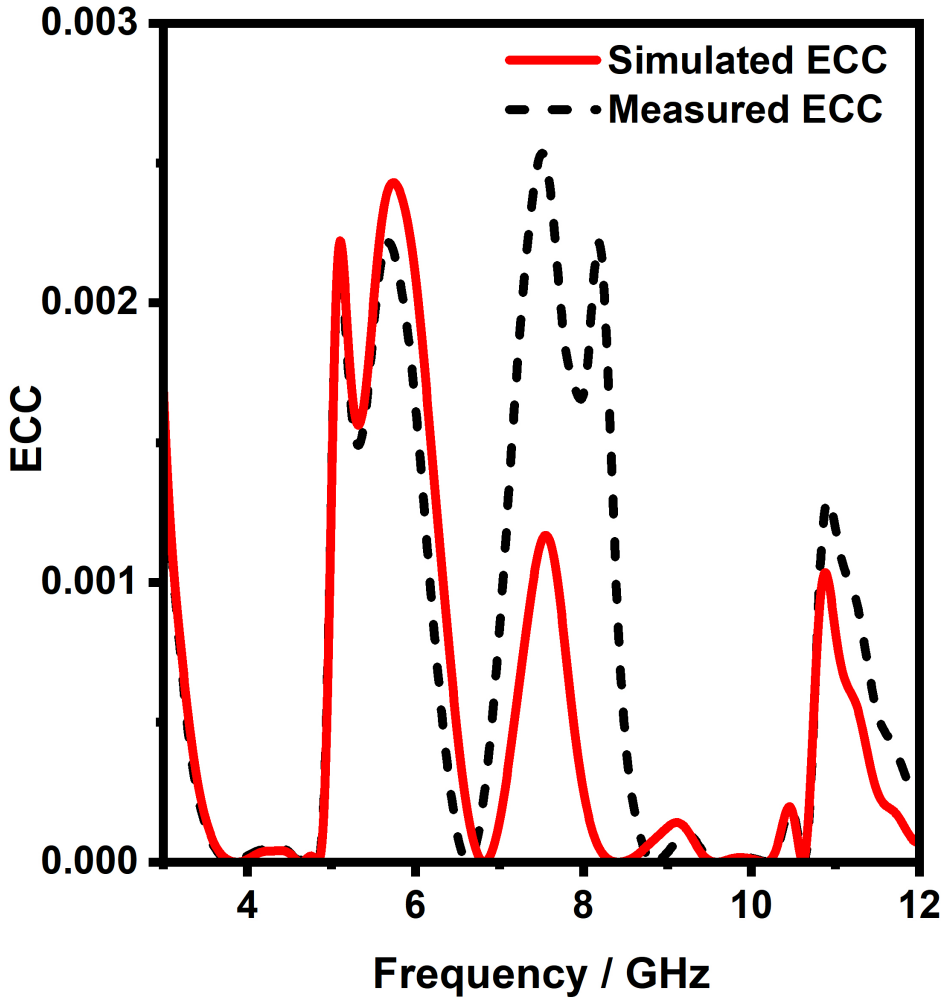

FIGURE 18: Simulated and measured ECC of the proposed MIMO antenna

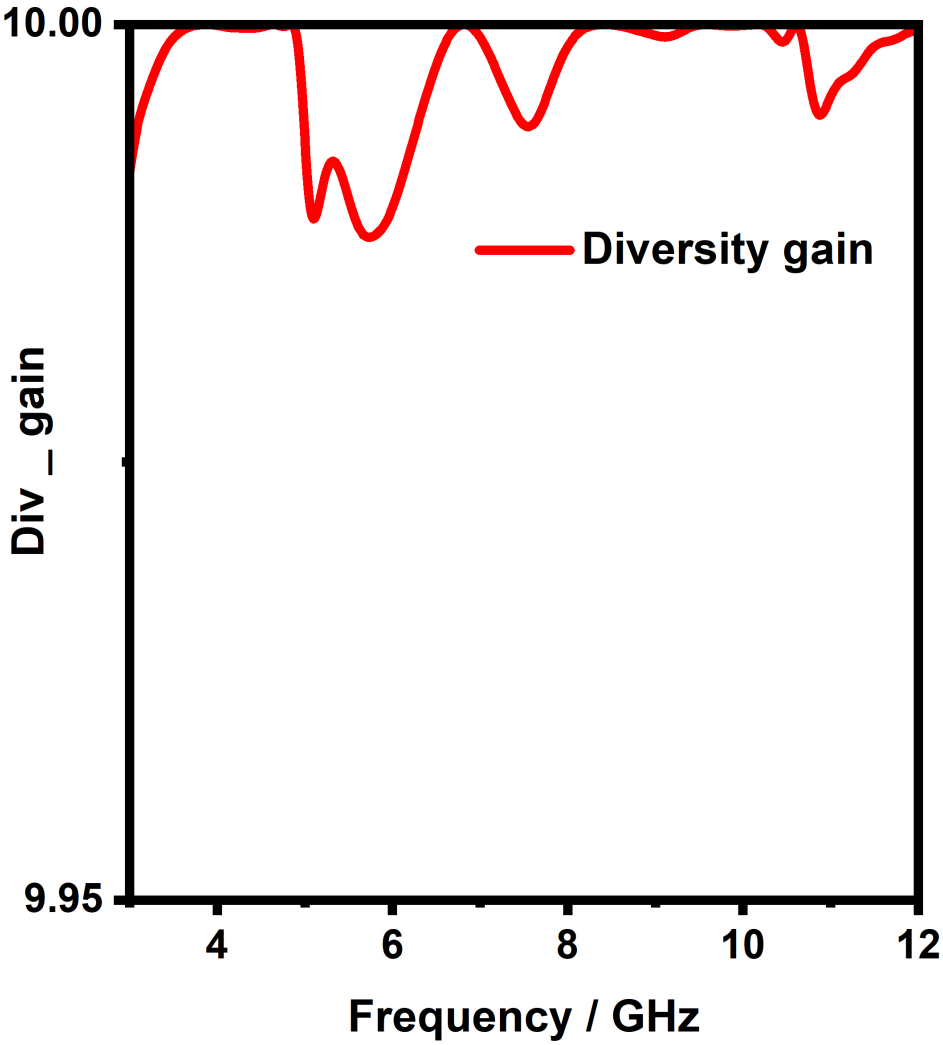

FIGURE 19: Simulated diversity gain of the proposed MIMO antenna

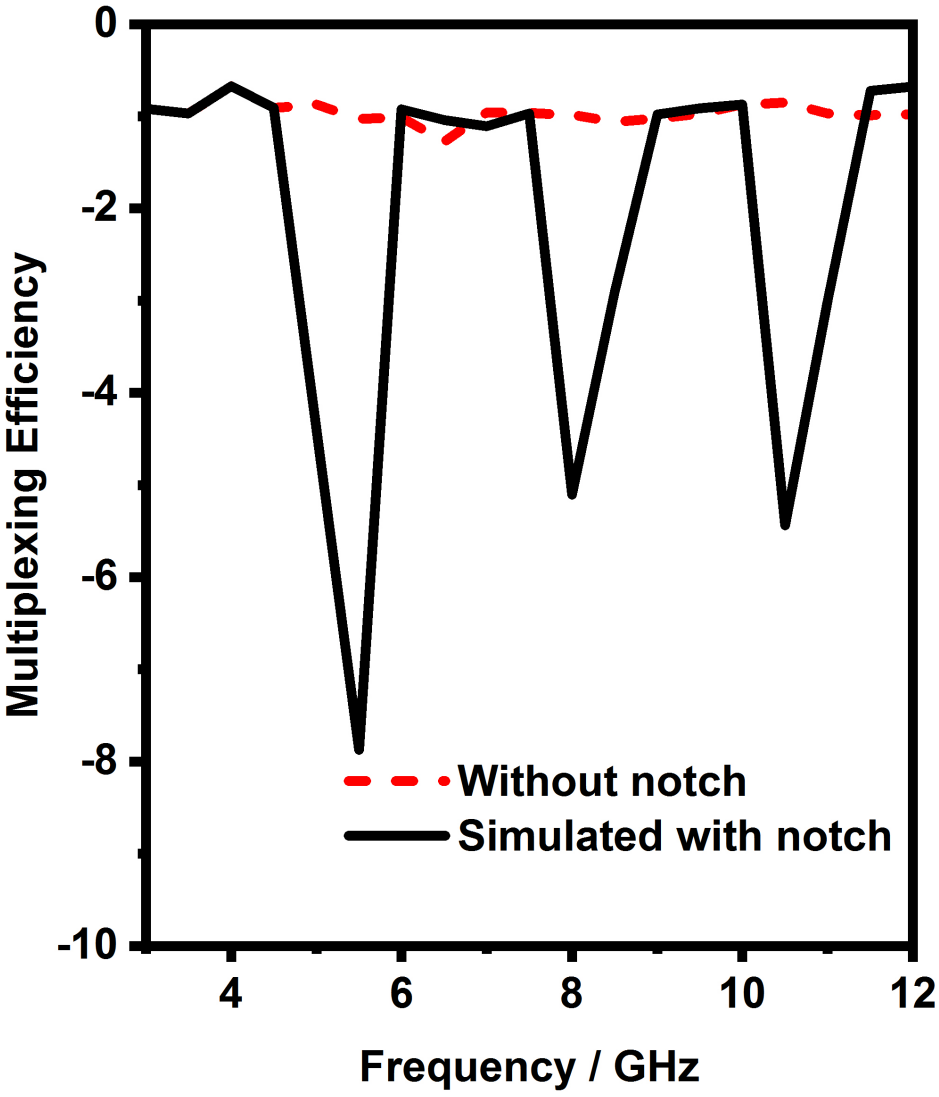

FIGURE 20: Simulated multiplexing efficiency of the proposed MIMO antenna

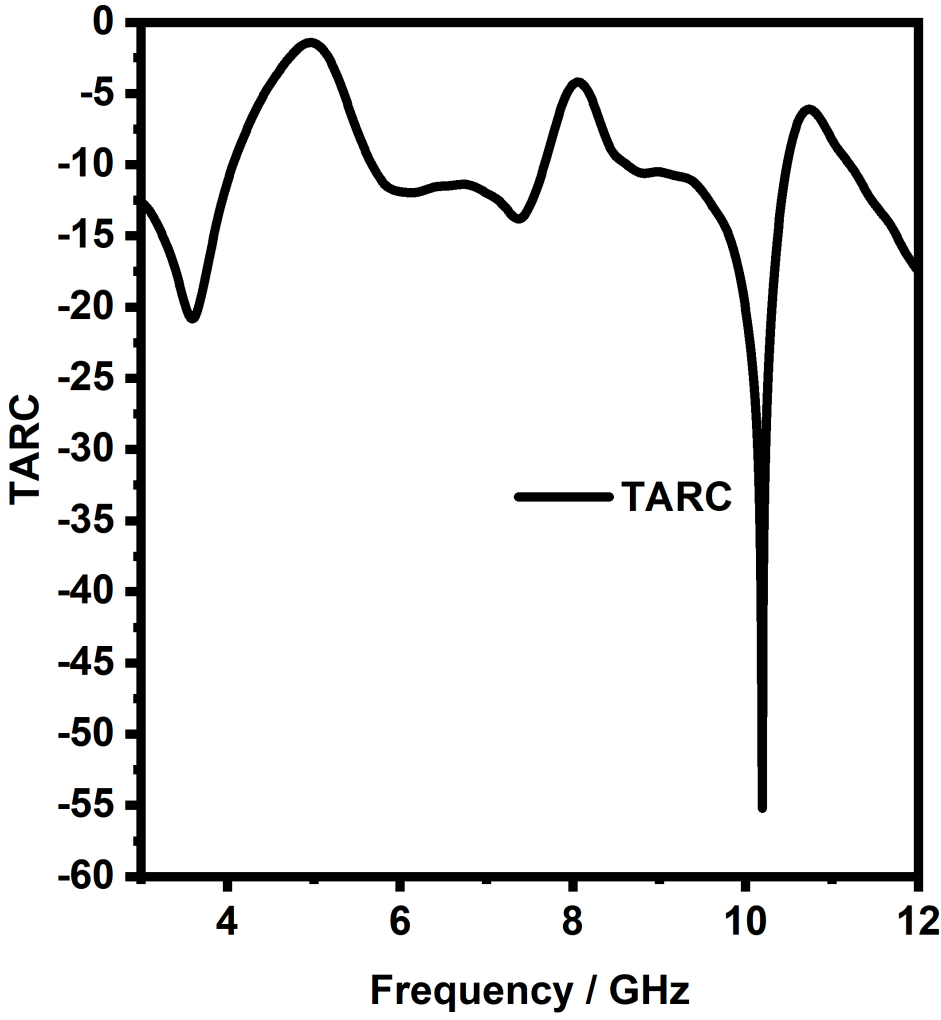

FIGURE 21: TARC for proposed MIMO antenna

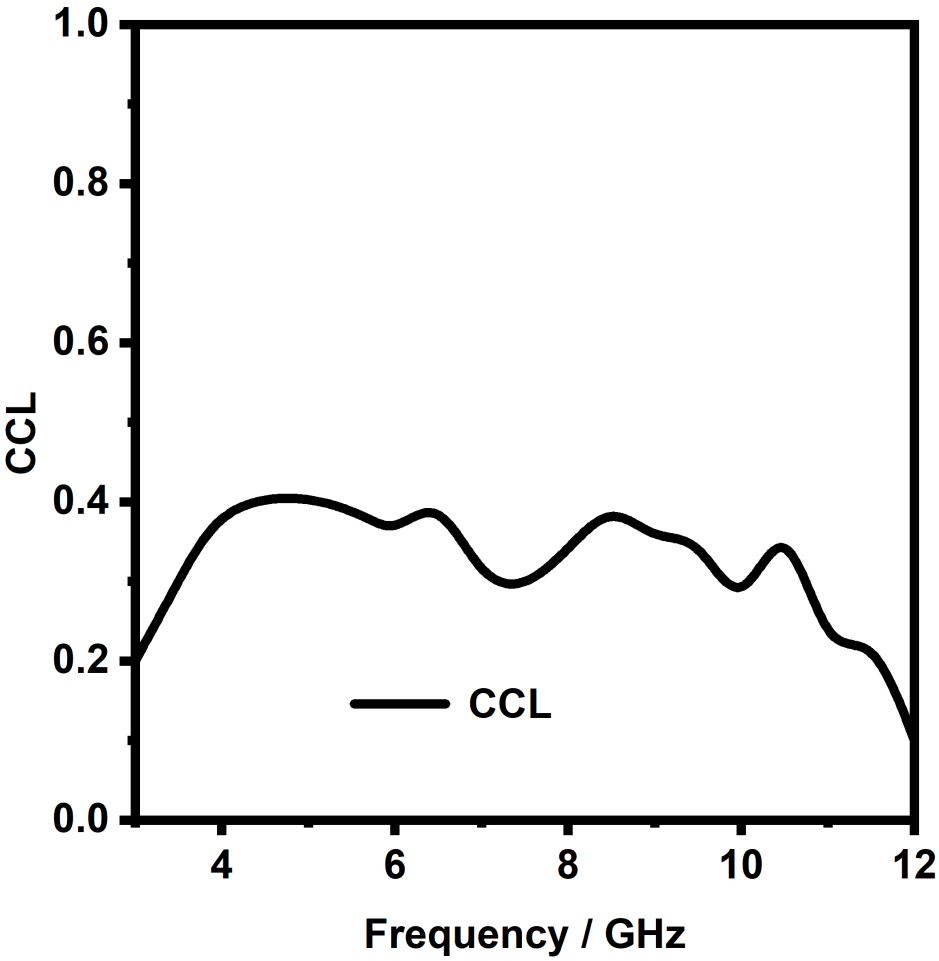

FIGURE 22: CCL of proposed MIMO antenna

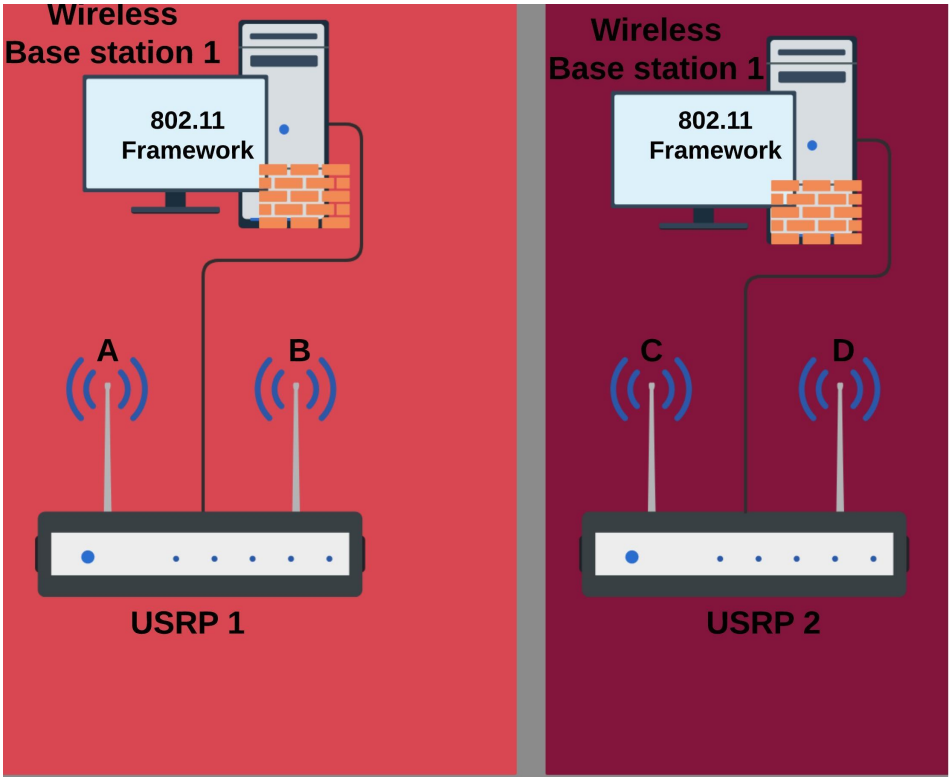

FIGURE 23: Block diagram of the indoor antenna test using USRP and 802.11 framework

FIGURE 24: Photograph of indoor base station environment using the proposed MIMO antenna; Received power and speed measurement in TxR and RxR streaming in 802.11 framework for case 1and case 2

List of Tables

TABLE 1
Comparison of existing antennas with proposed MIMO antenna

Ref	Number of elements	Size (mm^2)	Frequency (GHz)	Isolation(dB)	ECC	Gain(dBi)
[3]	2	27.2 × 46	3 -18	>18	0.018	1.5 -4.4
[4]	2	64 × 45	2-11	>15	0.02	-
[5]	2	50 × 30	2.5-15	>20	0.04	-
[6]	2	18 × 34	2-20	>22	0.01	0 - 7
[7]	2	18 × 34	2.5-12	>20	<0.02	0-4.2
[8]	2	68 × 38	2.4	>20	0.0002	2
[11]	4	70 × 70	2-14	>20	0.007	0-6
[12]	2	25 × 24	2.5 & 5.6	>20	0.15	0.28/3.88
[13]	2	18 × 36	2.8 - 20	>20	0.02	0-5
[14]	4	30 × 30	3-11	>20	0.04	0-7
[15]	4	40 × 40	3-11	>15	0.06	0-6
[16]	2	26 × 26	2-14	>16	0.02	0-7
[17]	4	39 × 39	2-14	>22	0.02	0-5
[19]	1	32 × 16.5	2 - 11	-	-	2
[22]	2/4	44 × 50	0-18	>20	0.1	-
[23]	4	40.5 × 40.5	3.1-10.6	>17	0.035	0-5
Prop	**2**	**18 × 28**	3-12	**>19**	**0.004**	0-7.5

TABLE 2
Proposed MIMO antenna Dimensions

P	D(mm)	P	D(mm)	P	D(mm)	P	D(mm)
W_R	7.75	L_f	6.5	W_{up}	7	L_{sr}	3
W_d	1.85	L_v	7.25	W_{lp}	4	W_{sr}	1.7
W_f	1.85	L_g	5	L_{up}	1.7	g_{sr1}	0.3
Wg	12	L_d	7.25	L_{lp}	1.7	g_{sr}	0.3
W	28	L_s	13	g_s, g_2	0.3	L_1	0.85
L	18	R_a	0.5	L_R	4	L_2	0.85

TABLE 3
Received power and throughput speed in NI lab view 802.11 framework

Mode	Tx	Rx	Distance	Received Power (dBm)	Throughput speed(Mb/s
			1	30	2.3
Case 1	A, B	C, D	1.5	35	1.5
			2	40	1.1
			1	30	2.3
Case 2	A, C	B, D	1.5	35	1.5
			2	40	1.1